The Classical Wave Equation: A Guide to Theoretical Concepts for Enhanced Student Understanding

Abstract. An intuitive guide for students' understanding of the one dimensional classical wave equation was developed. The objective was to bridge the gap between theoretical derivations and its practical applications, with particular emphasis on modeling the elastic properties of structures. Foundational principles and theoretical derivation were first introduced and extended into the application of Fourier series techniques to unravel deep concepts not explained in engineering mathematical textbooks that students find difficult to comprehend. Analytical and numerical methods were used to reinforce critical concepts that would have otherwise remained abstract outside the realm of demonstration and practical application. The numerical analysis aids with understanding the theory as it showed the evolution of wave patterns, which agreed with the analytical solution. The results obtained from comparing both analytical and numerical solutions show that different time step values (Δt) influenced the numerical solutions only by shifting the function, $f(x)$, in amplitude, but its shape and agreement with the analytical solution were maintained. This research demonstrates how innovative teaching techniques, which include the combined use of analytical and numerical methods, can be applied to improve students' understanding of mathematical theory and physical applications in engineering.

Keywords: Wave equation, Engineering Mathematics, Fourier series, Numerical Analysis, structural dynamics.

1 Introduction

Engineering mathematics is the cornerstone of various engineering disciplines, forming the bedrock upon which practical applications are built. At the heart of this mathematical framework lies the classical wave equation, which is a fundamental model that is crucial for comprehending wave propagation and vibrations. Integral to engineering education, the wave equation plays a pivotal role in Partial Differential Equations (PDEs) and Vector Calculus. Despite its significance, students often grapple with understanding its theoretical origins and practical implications. This paper addresses this challenge by aiming to enhance students' grasp of the classical wave equation's theoretical aspects and its connection to real-world applications. This involves synthesising the complete analytical solution with numerical methods while reviewing recent research contributing to a broader understanding of mathematical concepts.

For instance, a current shift in teaching differential equations (DEs) require visual interpretation of the solution space. This emphasises the need to adapt an analytical solution into a numerical form for enhanced student understanding. In response to the lack of studies on this approach Rezvanifard et al. [13] designed two collaborative tasks (sophism and paradox) for undergraduate engineering students. These tasks aimed to investigate students' understanding of exact DEs and to analyse their learning processes within small groups, which involved 135 undergraduate students. The findings highlight that engaged graphical-based learning facilitated a more conceptual grasp of the subject among students. This type of visual approach to learning was first proposed by [14] and [15] as visual cognitive learning theory.

Educational theories, such as those proposed by [16], advocate for a student-centered approach where learners take responsibility for constructing their own knowledge. This philosophy emphasises the importance of inductive reasoning as a means of fostering effective learning. According to Bruner, students actively engage in the learning process, constructing knowledge through exploration and discovery.

In a recent study by [11], the researchers investigated the intersection of effective learning in computational thinking (CT) and mathematics. Their findings revealed that the adoption of geometrised programming and student-centered instructional methods played a pivotal role in promoting effective learning. The study identified a dynamic and cyclical cognitive process inherent in CT-based mathematics learning, intertwining mathematical reasoning and computational thinking. Their work shed light on three key facets of this cognitive process: (1) Students actively apply mathematical principles while creating CT artifacts, showcasing a hands-on approach akin to Bruner's emphasis on active learning. (2) The study underscores the crucial role of mathematical principles in the anticipation and interpretation of CT-generated outputs, aligning with Bruner's emphasis on constructing knowledge through personal engagement. (3) Students concurrently develop new mathematical insights while engaging in CT activities. This echoes Bruner's philosophy, highlighting the parallel evolution of understanding and the interconnectedness of theory and numerical methods in students' learning outcomes.

The coupling of Bruner's student-centric philosophy, which underlines active engagement with the findings of [11] on the dynamic relationship between mathematical theory and computational thinking, provides a broader perspective on fostering effective learning in both mathematics and CT. This synthesis, complemented by the structured learning process inherent in Bloom's Taxonomy methods [18], [19], [17], underscores the significance of students actively constructing knowledge to align with the principles

advocated by Bruner. Furthermore, it is evident that educational disparities extend beyond subject domains. For instance, performance between male and female students in the realm of chemistry led educators to research initiatives aimed to address this gap. A notable investigation by [20] explored the impact of computer simulations on senior secondary school chemistry students, which focused specifically on gender differences. In a quasi-experimental design involving 83 participants, the study found a statistically significant main effect of treatment on overall student performance. Interestingly, despite this effect, no significant gender-based differences were identified. This suggests that the use of computer simulations holds promise in bridging performance gaps between male and female students in chemistry. The study's conclusions highlight the broader enhancement of student performance and advocate for the implementation of these findings through recommendations to governmental bodies, school administrators, and chemistry educators. Furthermore, the study encourages continued research in this domain to deepen our understanding and refine educational interventions.

With respect to the wave equation, Yang et al. [2] presented a study on functions of order one as solutions to the classical wave equation in a one-dimensional (1D) space. They proposed a conjecture suggesting that these functions have purely real zeros throughout the complex plane, offering an intriguing connection between number theory and wave equations. Wang and colleagues [3] introduced a fast guided wave imaging method based on convolutional neural networks (CNN) for corrosion mapping. This method allows for real-time prediction of corrosion damage thickness using guided wave data, which demonstrated high accuracy and resistance to noise. Walker et al. [4] developed VisualPDE as an online interactive solver for 1D and 2D partial differential equation (PDE) systems. VisualPDE enables instantaneous and interactive exploration of complex nonlinear systems, making it valuable for education and knowledge exchange in mathematical biology and related fields. Nagarajaiah [5] proposed the SimultaNeous Basis Function Approximation and Parameter Estimation (SNAPE) technique, which employs measured spatiotemporal responses to infer the governing PDEs. SNAPE demonstrates robust parameter estimation for PDEs, even in the presence of high noise levels, with applications ranging from Schrödinger equations to Navier-Stokes equations.

Ding et al. [6] studied the use of space–time fractional-order operators in simulating linear elastic waves in 1D periodic structures on viscoelastic foundations. They develop a homogenised model capable of capturing both material and geometric inhomogeneity and viscoelastic behavior. This method offered new insights into modeling wave dynamics and frequency band gaps. Chen et al. [7] proposed a physics-guided machine learning-based inverse design method for multifunctional wave control in active metabeams. The approach combined machine learning with transfer matrix method, providing a versatile means to design metamaterials with desired physical responses. Prieur et al. [8] studied a nonlinear 1D wave equation describing string deflection with distributed actuation subject to saturation. They establish well-posedness and asymptotic stability using nonlinear semigroups and Lyapunov techniques to showcase the importance of sector conditions in describing the saturating input. Lomovtsev and Spesivtseva [9] derive explicit solutions for a linear mixed problem in a general 1D wave equation with time-varying characteristic second derivatives in boundary conditions. Their work provides criteria for the well-posedness of the problem and emphasises data smoothness and consistency conditions. Guo et al. [10] addressed the error feedback regulator problem for the 1D wave equation with harmonic disturbance. They propose an adaptive control approach that achieves tracking error regulation and state boundedness by utilising measured tracking error and

disturbance parameter estimation.

In our case, we aimed to simplify the theoretical foundations of the classical wave equation by offering clear, step-by-step explanations for engineering students at the undergraduate level. To address the practical context the wave equation was related to a real-world scenario by characterising the elastic properties of a beam structure as an elastic string. Once this relationship was established, the analytical solution was converted to a numerical form in an effort to bridge theory and application. This served as a prerequisite and motivation for additional coursework on the discretisation of PDEs, where numerical methods are taught, to demostrate that theoretical concepts in engineering is not an abstract phenomenon but serves as the bedrock of all engineering principles and design.

1.1 The Wave Equation: A Theoretical Overview

To solve the wave equation, we often need to specify boundary conditions and initial conditions. The boundary conditions, given at $x = 0$ and $x = L$ in a one dimensional (1D) model is applied to help determine the first two arbitrary constants in the general solution. These conditions could be, for example, fixed ends ($u(0,t) = 0$ and $u(L,t) = 0$) or free ends ($\frac{\partial u}{\partial x}(0,t) = 0$ and $\frac{\partial u}{\partial x}(L,t) = 0$).

However, to fully solve the complete wave equation, the initial conditions has to be considered. These conditions specify the initial displacement, $u(x,0)$, and the initial velocity, $\frac{\partial u}{\partial t}(x,0)$, of the wave at $t = 0$. The wave equation is given by:

$$\frac{\partial^2 u}{\partial t^2} = c^2 \frac{\partial^2 u}{\partial x^2} \tag{1}$$

To solve (1), we aim to find a solution u that is not identically zero, satisfying boundary conditions, with the property that the dependence of u on x and t is separated. We assume a solution of the form $u(x,t) = X(x)T(t)$, where X is a function of x only, and T is a function of t only, such that the equivalent of each separable term equals a constant k. Separating variables, we obtain:

$$X'' = kX \tag{2}$$

$$T'' = c^2 kT \tag{3}$$

To obtain a solution a value, k, that satisfies the physical system has to be found.

1. If $k = 0$:

   From (2), $X'' = 0$, leading to $X = ax + b$. However, $X = 0$ at $x = 0$ and $x = l$, implying $a = 0$ and $b = 0$, resulting in $X = 0$, which is not oscillatory as required.

2. If k is positive, let $k = p^2$:

   From (2), $X'' - p^2 X = 0$, leading to the auxiliary equation $m^2 - p^2 = 0$. Solving this gives $m = \pm p$. Thus, the solution for X is:

   $$X = Ae^{px} + Be^{-px}$$

   However, $X = 0$ at $x = 0$ and $x = l$, implying $A = B = 0$, resulting in $X = 0$, which is not oscillatory as required.

3. If k is negative, let $k = -p^2$:

   From (2) and (3), $X'' + p^2X = 0$ and $T'' + c^2p^2T = 0$, leading to the following solutions that fit the requirements for an oscillatory function:

$$X = A\cos(px) + B\sin(px), \quad T = C\cos(cpt) + D\sin(cpt)$$

   Combining the spatial and temporal solutions, we get:

$$u(x,t) = XT = (A\cos(px) + B\sin(px))(C\cos(cpt) + D\sin(cpt))$$

   By setting $cp = \lambda$, simplifying further gives:

$$u(x,t) = (A\cos(px) + B\sin(px))(C\cos(\lambda t) + D\sin(\lambda t))$$

   where A, B, C, and D are arbitrary constants to be determined.

Now, we considered the boundary conditions:
(a) $u = 0$ when $x = 0$ for all values of t. This implies $A = 0$.
(b) $u = 0$ when $x = l$ for all values of t. This implies $\sin(pl) = 0$ and knowing that $\sin(n\pi) = 0$, then $pl = n\pi$, which gives $p_n = \frac{n\pi}{l}$ for $n = 1, 2, 3, \ldots$. Hence, the final solution is:

$$u(x,t) = B_n \sin\left(\frac{n\pi x}{l}\right)(C\cos(\lambda t) + D\sin(\lambda t))$$

where n is an integer, $p_n = \frac{n\pi}{l}$, and B_n is determined by the initial condition and Fourier techniques. This solution can be generalised as follows:

$$u(x,t) = \sum_{n=1}^{\infty} \sin\left(\frac{n\pi x}{l}\right)(C_n\cos(\lambda t) + D_n\sin(\lambda t)) \tag{4}$$

The next step is to determine the coefficients C_n and D_n by applying initial conditions:
(c) At $t = 0$, $u(x,0) = f(x)$ for $0 \le x \le l$. From our general solution for $n = 1, 2, 3, \ldots, r$, we have:

$$f(x) = \sum_{n=1}^{r} \sin\left(\frac{n\pi x}{l}\right)(C_n\cos(\lambda t) + D_n\sin(\lambda t)) \tag{5}$$

At $t = 0$, when $\cos(0) = 1$ and $\sin(0) = 0$, the equation simplifies to:

$$f(x) = \sum_{n=1}^{r} \sin\left(\frac{n\pi x}{l}\right) C_r \tag{6}$$

(d) Also, at $t = 0$, $\frac{\partial u}{\partial t}(x,0) = g(x)$ for $0 \le x \le l$. Differentiating the general solution with respect to t and set $t = 0$, which yields:

$$\frac{\partial u}{\partial t} = \sum_{r=1}^{r} \left(\frac{c\pi}{l} r \sin\left(\frac{r\pi x}{l}\right) D_r\cos(\lambda t) - \frac{c\pi}{l} r \sin\left(\frac{r\pi x}{l}\right) C_r\sin(\lambda t)\right) \tag{7}$$

Now, applying $\frac{\partial u}{\partial t}(x,0) = g(x)$ at $t = 0$,

$$g(x) = \sum_{r=1}^{r} \frac{c\pi}{l} r \sin\left(\frac{r\pi x}{l}\right) D_r \tag{8}$$

With initial boundary conditions satisfied, the coefficients C_r and D_r from equations (6) and (8) can be determined using Fourier series and the orthogonality of functions.

Derivation of Fourier Sine Series Coefficients

To determined the coefficients C_r and D_r that make $u(x,0)$ and $\frac{\partial u}{\partial t}(x,0)$, using the Fourier sine series of $f(x)$ and $g(x)$, respectively, gives:

$$u(x,0) = \sum_{r=1}^{\infty} C_r \sin\left(\frac{r\pi x}{L}\right) = f(x) \tag{9}$$

and

$$u(x,0) = \frac{c\pi}{L} \sum_{r=1}^{\infty} D_r \; r \sin\left(\frac{r\pi x}{L}\right) = g(x) \tag{10}$$

The result obtained are as follows:

$$C_r = \frac{2}{L} \int_0^L f(x) \; sin \frac{r\pi x}{L} \, dx \quad r = 1, 2, 3, \ldots \tag{11}$$

and

$$D_r = \frac{2}{rc\pi} \int_0^L g(x) \; sin \frac{r\pi x}{L} \, dx \quad r = 1, 2, 3, \ldots \tag{12}$$

To determine coefficients C_r and D_r in equations (11) and (12), in relation to (9) and (10), the orthogonality property of Fourier series was used. First, both sides of (9) are multiplied by $\sin\left(\frac{m\pi x}{L}\right)$ and integrate over the interval $[0, L]$:

$$\int_0^L C_r \sin\left(\frac{n\pi x}{L}\right) \left[\sin\left(\frac{m\pi x}{L}\right)\right] dx = \int_0^L f(x) \left[\sin\left(\frac{m\pi x}{L}\right)\right] dx \tag{13}$$

Using the orthogonality property of sine functions, all terms except the one with $n = m$ (corresponding to the same eigenvalue) will integrate to zero.

Note: The orthogonality property of sine functions states that the sine functions are orthogonal (perpendicular) to each other over certain intervals (Stroud and Booth, 2007). Specifically, for two distinct positive integers m and n, the following property holds:

$$\int_0^L \sin\left(\frac{n\pi x}{L}\right) \sin\left(\frac{m\pi x}{L}\right) \, dx = \begin{cases} 0 & \text{if } m \neq n \\ \frac{L}{2} & \text{if } m = n \end{cases} \tag{14}$$

This property implies that when two different sine functions are multiplied and integrated over a certain interval, the result is zero, indicating their orthogonality. However, when the two sine functions have the same frequency (i.e., when $m = n$), the integral evaluates to $\frac{L}{2}$. Hence, from equation (13), w.r.t (14), we have:

$$\int_0^L C_r \sin^2\left(\frac{m\pi x}{L}\right)\, dx = \int_0^L f(x)\sin\left(\frac{m\pi x}{L}\right)\, dx \tag{15}$$

On the **LHS**, after solving the integral, (see **Appendix** for derivation). we see:

$$\int_0^L C_r \sin^2\left(\frac{m\pi x}{L}\right)\, dx = \frac{L}{2}B_m \tag{16}$$

and on the **RHS**, we have:

$$\int_0^L f(x)\sin\left(\frac{m\pi x}{L}\right)\, dx \tag{17}$$

Therefore, by combining (16) and (17), equation (15), becomes:

$$\frac{L}{2}C_r = \int_0^L f(x)\sin\left(\frac{m\pi x}{L}\right)\, dx \tag{18}$$

To find the coefficient C_r, we divide both sides by $\frac{L}{2}$ or multiply by its conjugate, $\frac{2}{L}$, to obtain:

$$C_r = \frac{2}{L}\int_0^L f(x)\sin\left(\frac{m\pi x}{L}\right)\, dx \tag{19}$$

This equation provides the formula to calculate the coefficients C_r based on the given initial displacement function $f(x)$ over the length of the interval L.

Hence, Fourier series can be used to find the two arbritrary constants C_r and D_r as the final solution, in (20), for the Wave equation.

$$\begin{aligned} u(x,t) = \sum_{r=1}^{\infty} \sin\frac{r\pi a}{L}\Bigg(&\left[\frac{2}{L}\int_0^L f(a)\sin\frac{r\pi a}{L}\, da\right]\cos\frac{rc\pi t}{L} \\ &+ \left[\frac{2}{rc\pi}\int_0^L g(a)\sin\frac{r\pi a}{L}\, da\right]\sin\frac{rc\pi t}{L}\Bigg) \end{aligned} \tag{20}$$

Note, $f(a)$ and $g(a)$ are used as initial conditions in the final result. The variable of integration (a) is now used instead of x to avoid confusion with (x) in $u(x,t)$.

2 Wave Propagation in a 1D Steel Beam

The aim is to model a beam as a 1D string to understand its elastic properties and wave propagation behaviour as an application of the theoretical foundation. Consider a 1D steel beam with a length of 20 cm subjected to the following conditions as illustrated in Figure 1 and equations [21 - 24].

$$u(0,t) = 0 \qquad \text{(fixed end point at } x = 0) \tag{21}$$

$$u(20,t) = 0 \qquad \text{(fixed end point at } x = 20) \tag{22}$$

$$u(x,0) = f(x) \qquad \text{(initial vertical displacement profile)} \tag{23}$$

$$\frac{\partial u}{\partial t}(x,0) = 0 \qquad \text{(zero initial velocity)} \tag{24}$$

The initial displacement profile $f(x)$ due to an imposed excitation is defined as follows:

$$f(x) = \begin{cases} \frac{x}{10} & \text{if } 0 \leq x \leq 10 \\ 2 - \frac{x}{10} & \text{if } 10 \leq x \leq 20 \end{cases}$$

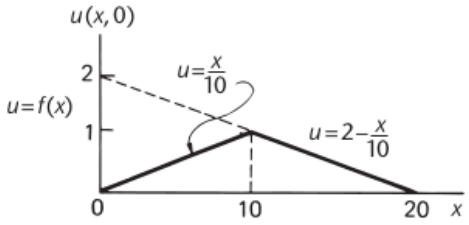

Figure 1: The analytical problem. *Source*: [1]

To solve this example problem, the method of separation of variables was applied and then Fourier series was used to expand $f(x)$ into a sum of sine functions. This allowed for determining the coefficients using the given boundary and initial conditions.

2.1 Analytical Solution

Implementing the theoretical solution, the eigenvalues and eigenfunctions were obtained in (25) and (26), where P_n and Q_n represent the coefficients for initial displacement and initial velocity, such that $P = B * C$ and $Q = B * D$.

$$\text{Eigenvalues:} \quad \lambda_n = \frac{n\pi}{20} \tag{25}$$

$$\text{Eigenfunctions:} \quad u_n(x,t) = \sin\frac{n\pi x}{20}\left(P_n \cos\frac{n\pi t}{20} + Q_n \sin\frac{n\pi t}{20}\right) \tag{26}$$

Applying initial condition $u(x,0) = f(x)$ results in (27) since $sin(0) = 0$ and $cos(0) = 1$

$$u_n(x,0) = f(x) = \sum_{n=1}^{\infty} P_n \sin\left(\frac{n\pi x}{20}\right) \tag{27}$$

To determine P_n from $f(x)$ in (27), Fourier techniques were applied, and then integrate by parts, since they are dissimilar functions. The complete integral for P_n is shown in (28), (29)

$$P_n = \frac{2}{20}\int_0^{20} f(x_1)\cdot\sin\left(\frac{n\pi x}{20}\right) + \frac{2}{20}\int_0^{20} f(x_2)\cdot\sin\left(\frac{n\pi x}{20}\right)dx \tag{28}$$

$$10P_n = \int_0^{10}\frac{x}{10}\cdot\sin\left(\frac{n\pi x}{20}\right)dx + \int_{10}^{20}\frac{20-x}{10}\cdot\sin\left(\frac{n\pi x}{20}\right)dx \tag{29}$$

Using integration by parts to solve for $f(x_1)$,

$$u = \frac{x}{10} \Rightarrow du = \frac{1}{10}dx, \quad dv = \sin\left(\frac{n\pi x}{20}\right)dx \Rightarrow v = -\frac{20}{n\pi}\cos\left(\frac{n\pi x}{20}\right)$$

$$f(x_1) = uv - \int v\,du = \left[\frac{x}{10}\cdot -\frac{20}{n\pi}\cos\left(\frac{n\pi x}{20}\right)\right]_0^{10} - \int_0^{10} -\frac{20}{n\pi}\cos\left(\frac{n\pi x}{20}\right)\cdot\frac{1}{10}dx$$

$$f(x_1) : uv = \frac{10}{10} \cdot \left(-\frac{20}{n\pi}\right) \cos\left(\frac{n\pi \cdot 10}{20}\right) - \frac{0}{10} \cdot \left(-\frac{20}{n\pi}\right) \cos\left(\frac{n\pi \cdot 0}{20}\right)$$

$$= -\frac{20}{n\pi} \cos\left(\frac{n\pi}{2}\right) - 0 = -\frac{20}{n\pi} \cos\left(\frac{n\pi}{2}\right)$$

$$f(x_1) : vdu = -\int_0^{10} \left(-\frac{20}{n\pi}\right) \cos\left(\frac{n\pi x}{20}\right) \cdot \frac{1}{10} dx = \frac{2}{n\pi} \int_0^{10} \cos\left(\frac{n\pi x}{20}\right) dx$$

$$= \frac{2}{n\pi} \cdot \frac{20}{n\pi} \left[\sin\left(\frac{n\pi x}{20}\right)\right]_0^{10} = \frac{2}{n\pi} \cdot \frac{20}{n\pi} \left[\sin\left(\frac{n\pi}{2}\right) - \sin(0)\right] = \frac{40}{n^2\pi^2} \sin\left(\frac{n\pi}{2}\right)$$

$$f(x_1) = -\frac{20}{n\pi} \cos\left(\frac{n\pi}{2}\right) + \frac{40}{n^2\pi^2} \sin\left(\frac{n\pi}{2}\right) \tag{30}$$

For $f(x_2)$,

$$f(x_2) = uv - \int v\, du = \left[\frac{20 - x}{10} \cdot -\frac{20}{n\pi} \cos\left(\frac{n\pi x}{20}\right)\right]_{10}^{20} + \frac{2}{n\pi} \int_{10}^{20} \cos\left(\frac{n\pi x}{20}\right) dx$$

where:

$$u = \frac{20 - x}{10} \Rightarrow du = -\frac{1}{10} dx, \quad dv = \sin\left(\frac{n\pi x}{20}\right) dx \Rightarrow v = -\frac{20}{n\pi} \cos\left(\frac{n\pi x}{20}\right)$$

$$f(x_2) : uv = \left(\frac{20 - 20}{10} \cdot -\frac{20}{n\pi} \cos\left(\frac{n\pi \cdot 20}{20}\right)\right) - \left(\frac{20 - 10}{10} \cdot -\frac{20}{n\pi} \cos\left(\frac{n\pi \cdot 10}{20}\right)\right)$$

$$= 0 - \left(-\frac{20}{n\pi} \cos\left(\frac{n\pi}{2}\right)\right) = \frac{20}{n\pi} \cos\left(\frac{n\pi}{2}\right)$$

$$f(x_2) = \frac{2}{n\pi} \int_{10}^{20} \cos\left(\frac{n\pi x}{20}\right)\, dx = \frac{2}{n\pi} \left[\frac{20}{n\pi} \sin\left(\frac{n\pi x}{20}\right)\right]_{10}^{20}$$

$$= \frac{2}{n\pi} \left(\frac{20}{n\pi} \sin\left(\frac{n\pi \cdot 20}{20}\right) - \frac{20}{n\pi} \sin\left(\frac{n\pi \cdot 10}{20}\right)\right)$$

$$= \frac{40}{n^2\pi^2} \left(\sin(n\pi) - \sin\left(\frac{n\pi}{2}\right)\right)$$

$$= \frac{40}{n^2\pi^2} \left(2 \sin\left(\frac{n\pi}{2}\right) - \sin\left(\frac{n\pi}{2}\right)\right)$$

$$f(x_2) = \frac{20}{n\pi} \cos\left(\frac{n\pi}{2}\right) + \frac{40}{n^2\pi^2} \left(2 \cdot \sin\left(\frac{n\pi}{2}\right) - \sin\left(\frac{n\pi}{2}\right)\right) \tag{31}$$

Therefore, for $n = 1, 2, 3 \ldots$, the complete solution for $10P_n = f(x_1) + f(x_2)$ is:

$$= \left[-\frac{20}{n\pi} \cos\left(\frac{n\pi}{2}\right) + \frac{40}{n^2\pi^2} \sin\left(\frac{n\pi}{2}\right) \right] + \left[\frac{20}{n\pi} \cos\left(\frac{n\pi}{2}\right) + \frac{40}{n^2\pi^2} \left(2 \cdot \sin\left(\frac{n\pi}{2}\right) - \sin\left(\frac{n\pi}{2}\right) \right) \right]$$

$$10P_n = \frac{40}{n^2\pi^2} \left(2 \cdot \sin\left(\frac{n\pi}{2}\right) \right)$$

$$P_n = \frac{40}{n^2\pi^2} \left(2 \cdot \sin\left(\frac{n\pi}{2}\right) \right) \cdot \frac{1}{10}$$

$$P_n = \frac{8}{\pi^2 r^2} \sin\frac{r\pi}{2} \tag{32}$$

Substituting equation P_n from (32) in (26), $u(x,t)$ becomes:

$$u_n(x,t) = \sin\frac{n\pi x}{20} \left(\frac{8}{\pi^2 r^2} \sin\frac{r\pi}{2} \cos\frac{n\pi t}{20} + Q_n \sin\frac{n\pi t}{20} \right) \tag{33}$$

Also, at $\frac{\partial u}{\partial t}\big|_{t=0}$,

$$\frac{\partial u_n}{\partial t} = \sin\frac{n\pi x}{20} \left(\frac{8}{\pi^2 r^2} \sin\frac{r\pi}{2} \left(-\frac{n\pi}{20} \right) \sin\frac{n\pi t}{20} + Q_n \frac{n\pi}{20} \cos\frac{n\pi t}{20} \right)$$

Substituting $t = 0$ into the expression:

$$\left.\frac{\partial u_n}{\partial t}\right|_{t=0} = \sin\frac{n\pi x}{20} \left(\frac{8}{\pi^2 r^2} \sin\frac{r\pi}{2} \left(-\frac{n\pi}{20} \right) \sin 0 + Q_n \frac{n\pi}{20} \cos 0 \right)$$

Simplifying further:

$$\left.\frac{\partial u_n}{\partial t}\right|_{t=0} = \sin\frac{n\pi x}{20} \left(0 + Q_n \frac{n\pi}{20} \cdot 1 \right) = \frac{n\pi}{20} Q_n \sin\frac{n\pi x}{20}$$

Here, Q_n represents the amplitude of the n-th mode and can be zero for certain modes (as in the case $Q_n = 0, n = 20$). This means those modes do not contribute to the overall solution as the presence or absence of a specific Q_n term affects the shape and behavior of the wave. The sine function, $\sin(\pi x)$, is a periodic function with values ranging between -1 and 1. The product of πQ_{20} and $\sin(\pi x)$ can be equal to zero for certain values of x. Considering the equation

$$0 = \frac{n\pi}{20} Q_n \sin\frac{n\pi x}{20}$$

and assuming n and π are nonzero constants, for this equation to hold for all x, Q_n must be equal to zero. Consequently, $Q_{20} = 0$. It's important to note that when $n = 20$, the equation becomes,

$$0 = \pi Q_{20} \sin(\pi x)$$

and implies that the contribution of n=20 mode is absent in the overall solution. Therefore, the entire equation simplifies to $0 = 0 \times \sin(\pi x)$, which is indeed true for any value of x. Thus, the final solution becomes:

$$u(x,t) = \frac{8}{\pi^2} \sum_{n=1}^{\infty} \frac{1}{r^2} \sin\left(\frac{r\pi x}{20}\right) \sin\frac{r\pi}{2} \cos\frac{r\pi t}{20} \tag{34}$$

The significance of $Q_{20} = 0$ in this context was discussed as it implies that the term associated with $n = 20$ in the Fourier series solution for the wave equation is zero. This means the solution can be accurately represented without the need for a term associated with $n = 20$.

3 Numerical Implementation

To convert the analytical solution into a numerical form, the finite difference method was employed, which is a widely used technique for solving partial differential equations. The spatial and temporal domains were both discretised to approximate the solution. For the spatial domain, the steel structure was divided into a set of discrete spatial points, creating a uniform grid with a spatial resolution denoted as N_x. The spatial step size was calculated as $\Delta x = \frac{L}{N_x}$. Similarly, for the temporal domain, time was discretised into discrete time steps with a temporal resolution represented as N_t, and the time step size was calculated as $\Delta t = \frac{T}{N_t}$ for the analytical solution in (34).

A 2D array u with dimensions (N_x, N_t) was initialised to store the values of displacement at each spatial point and time step. The initial condition $u(x, 0)$ was set based on the $f(x)$ profile. The central difference scheme was implemented to update the values of u at each time step. This scheme approximated the second-order spatial and temporal derivatives and iterated over time steps and spatial points. To visualise the results, plots of displacement u were created at different time steps. These plots allowed us to observe the propagation of waves and different modes in the steel structure.

4 Results and Discussion

Figure 2 illustrates the numerical simulation of the wave equation for different time steps. To validate the effectiveness of the approach the numerical output was compared with the results of the analytical solution obtained in equations (32) and (34), shown at a single reference point in Figure (3).

Table 1: Comparison of Analytical and Numerical Solutions at $x = 10$, $t = 5$ for Different Δt Values

Δt	Analytical Solution	Numerical Solution
1	3.7525649177131846	5.9939659838946815
2	3.7525649177131846	2.9969841893093094
3	3.7525649177131846	1.9979907907907908
4	3.7525649177131846	1.9979851851851853
5	3.7525649177131846	1.997977977977978
6	3.7525649177131846	0.998998998998999

To further understand and verify the results, the wave propagation, with a particular focus on the impact of different time step sizes (Δt), was studied. The results were recorded in Table (1). The objective was to obtain agreement between the analytical

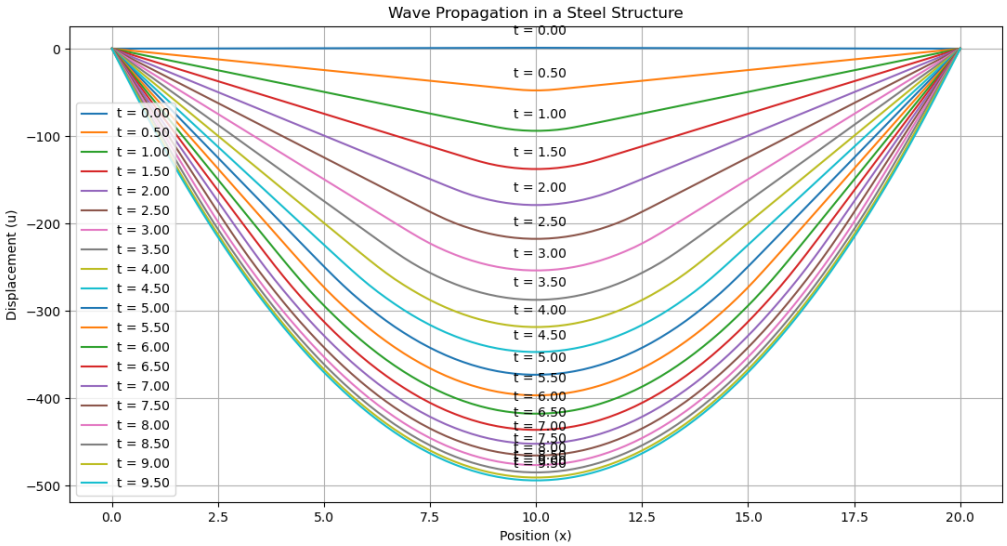

Figure 2: Numerical simulations illustrating the evolution of wave patterns.

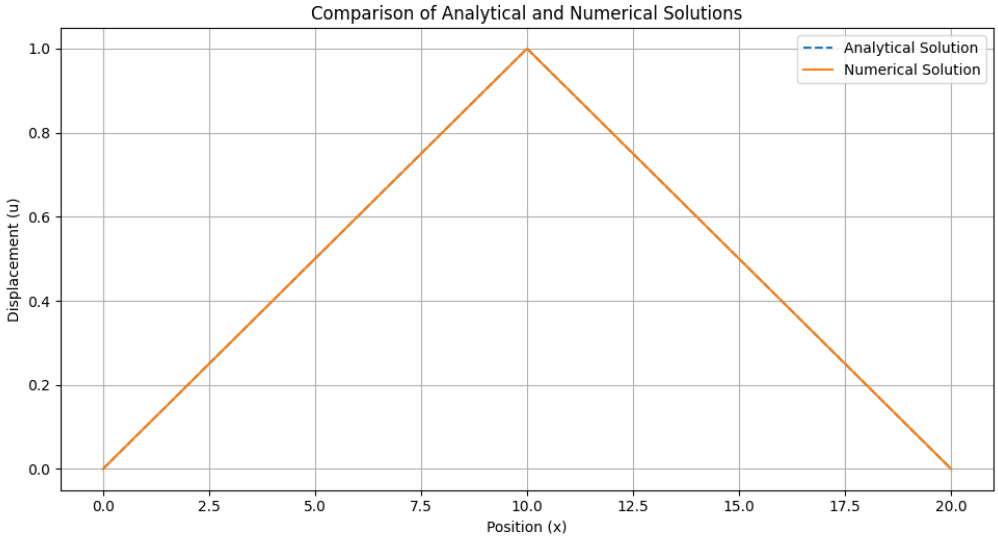

Figure 3: Step size = 3, x-location=5.

and numerical solutions, ensuring that the shape of the curves aligns with the problem at hand. The analytical solution served as reference to which the numerical results can be compared with. It was based on a series of terms (P_n) and a double summation to provide an exact representation of the wave propagation in the steel structure even at varying time steps as shown in Figures 4.

To achieve agreement between the analytical and numerical solutions, a central difference scheme was used. The finite difference scheme was applied to discretise the partial differential equation governing wave propagation. The idea was to incrementally vary the time step size (Δt) while keeping other parameters constant.

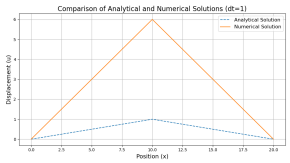

(a) $\Delta t = 1$

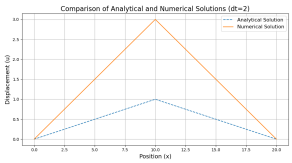

(b) $\Delta t = 2$

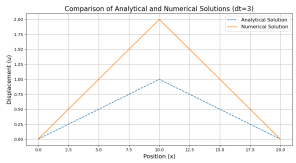

(c) $\Delta t = 3$

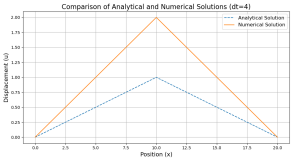

(d) $\Delta t = 4$

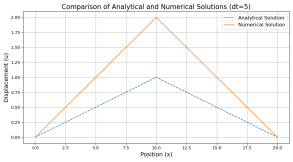

(e) $\Delta t = 5$

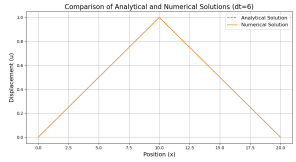

(f) $\Delta t = 6$

Figure 4: Comparison of Analytical and Numerical Solutions at $x = 10$, $t = 5$ for Different Δt Values

4.1 Impact of Δt on Results

One of the key observations was that different Δt values indeed yielded different results when compared. As Δt increased, there was a significant impact on the numerical solution. Specifically, larger Δt values led to better alignment of the curves in the analytical and numerical solutions. In contrast, smaller Δt values produced plot results with a higher amplitude for the numerical solution than that of the analytical solution.

Also, while the amplitude of the curves in the numerical solutions varied with different Δt values, the shape of the curves consistently adhered to the prescribed boundary conditions. This is a vital finding, as it implies that the fundamental physics of wave propagation in the steel structure remained intact. Despite variations in amplitude, the waveforms exhibited the expected behavior in terms of their spatial and temporal evolution.

Figure 3, showed the agreement between the analytical and numerical solutions at a specific spatial position ($x = 10$) and time ($t = 5$). This is in line with previous discussion. Varying the Δt values from 1 to 6 captured the changing behavior of the numerical solution. It is evident that larger Δt values, as seen in Figure (4) f, provided results that closely matched the analytical solution, both in terms of shape and amplitude. As Δt decreased, however, the amplitude of the numerical solution exhibited larger deviations from the analytical curve, but maintained expected shape of the curve function.

This underscores the significance of careful consideration when selecting time step sizes in numerical simulations. While larger time steps may offer computational advantages, they can lead to inaccuracies in capturing the physics of the problem. Future work may involve a more thorough exploration of the numerical stability and convergence properties of the chosen finite difference scheme. This would provide better insights into the variation in amplitudes experienced with variation in the temporal resolution.

5 Conclusion

This study underscores the significance of achieving not only agreement between analytical and numerical solutions but also maintaining consistency in modeling physical behavior. Examination of different Δt values, illustrated the trade-offs between

computational efficiency and solution accuracy in the context of wave propagation. It emphasises the critical intersection of theoretical principles and practical applications within the realm of engineering mathematics, with a primary focus on enhancing the educational experience for students. In this context, there are several noteworthy contributions:

1. The analysis effectively demonstrated the relationship between theoretical derivations and their practical applications, bridging the gap between abstract mathematical concepts and real-world scenarios.

2. The utilisation of Fourier series techniques in solving the classical wave equation, coupled with boundary and initial conditions and integration by parts, has been showcased as a powerful tool in engineering mathematics.

3. The computation successfully implemented both analytical and numerical methods to unravel intricate problems in engineering, providing students with valuable problem-solving skills.

4. Through numerical simulations, the practical effectiveness of theoretical concepts in addressing complex engineering challenges were highlighted. This approach offers students a tangible understanding of theoretical principles in action.

References

[1] Stroud, K. A., & Booth, D. J. (2007). *Engineering Mathematics* (6th ed.). Macmillan International Higher Education. ISBN: 978-1-4039-4454-9.

[2] Yang, X.-j., Alsolami, A., & Ali, A. (2023). An even entire function of order one is a special solution for a classical wave equation in one-dimensional space. *Thermal Science*.

[3] Wang, X., Lin, M., Li, J., Tong, J., Huang, X., Liang, L., Fan, Z., & Liu, Y. (2022). Ultrasonic guided wave imaging with deep learning: Applications in corrosion mapping. *Mechanical Systems and Signal Processing*.

[4] Walker, B. J., Townsend, A., Chudasama, A. K., & Krause, A. L. (2023). VisualPDE: rapid interactive simulations of partial differential equations.

[5] Nagarajaiah, S. (2021). Data-Driven Theory-Guided Learning of Partial Differential Equations Using Simultaneous Basis Function.

[6] Ding, W., Hollkamp, J. P., Patnaik, S., & Semperlotti, F. (2022). On the fractional homogenization of one-dimensional elastic metamaterials with viscoelastic foundation. *Archive of Applied Mechanics*.

[7] Chen, J., Chen, Y., Xu, X., Zhou, W., & Huang, G. (2022). A physics-guided machine learning for multifunctional wave control in active metabeams. *Extreme Mechanics Letters*.

[8] Prieur, C., Tarbouriech, S., Gomes da Silva, J. M., & Gomes da Silva, J. M. (2014). Well-posedness and stability of a 1D wave equation with saturating distributed input. *IEEE Conference on Decision and Control*.

[9] Lomovtsev, F. E., & Spesivtseva, K. A. (2021). Mixed problem for a general 1D wave equation with characteristic second derivatives in a nonstationary boundary mode. *Mathematical Notes*.

[10] Guo, W., Zhou, H., & Krstic, M. (2018). Adaptive error feedback regulation problem for 1D wave equation. *International Journal of Robust and Nonlinear Control*.

[11] Ye, H., Liang, B., Ng, O. L., et al. (2023). Integration of computational thinking in K-12 mathematics education: a systematic review on CT-based mathematics instruction and student learning. *IJ STEM Ed*, 10(3). https://doi.org/10.1186/s40594-023-00396-w

[12] Teaching Mathematics and its Applications: An International Journal of the IMA, Volume 42, Issue 2, June 2023, Pages 126–149. https://doi.org/10.1093/teamat/hrac005.

[13] Rezvanifard, F., Radmehr, F., & Rogovchenko, Y. (2023). Advancing engineering students' conceptual understanding through puzzle-based learning: a case study with exact differential equations. *Teaching Mathematics and its Applications: An International Journal of the IMA*, 42(2), 126–149. https://doi.org/10.1093/teamat/hrac005.

[14] Fleming, N. D., & Mills, C. (1992). Not another inventory, rather a catalyst for reflection. *To Improve the Academy*, 11(1), 137–155. Wiley Online Library.

[15] Fleming, N., Baume, D., & others. (2006). Learning Styles Again: VARKing up the right tree! *Educational Developments*, 7(4), 4. SEDA.

[16] Bruner, J. S. (1966). *Toward a Theory of Instruction*. Harvard University Press.

[17] Banda, S., Phiri, F., Kaale, J., Banda, A. M., Chikopela, D. L., Mpolomoka, R., & Mushibwe, C. (2023). Application of Bloom's Taxonomy in Categorization of Cognitive Process Development in Colleges.

[18] McGrath, M., Willcutt, W. (2022). The creative use of Thinking Maps to embed Bloom's Taxonomy within teaching, learning, and assessment. *Educatio: Jurnal Pendidikan STAIM Nganjuk*, 6(4), 346–372. Publisher: Sekolah Tinggi Agama Islam Miftahul Ula Nganjuk.

[19] Bunt, B. J., Grosser, M., van Tonder, D. (2022). A Novel Proposal to Use Thinking Maps to Embed Blooms' Taxonomy Within Teaching, Learning, and Assessment. *Journal of Cognitive Education and Psychology*. Publisher: Springer.

[20] Oladejo, A. I., Nwaboku, N. C., Okebukola, P. A., & Ademola, I. A. (2023). Gender difference in students' performance in chemistry–can computer simulation bridge the gap? *Research in Science & Technological Education*, 41(3), 1031–1050. Publisher: Taylor & Francis.

Funding
No funding was obtained for this research.

Appendix 1

Algorithm 1 Numerical Implementation Pseudocode

Initialisation:
Define constants:
L: Length of the steel structure
Nx: Number of spatial points
Nt: Number of time steps
dt: Temporal step size
Create a 2D array u with dimensions (Nx, Nt) to store displacements
Set Initial Condition:
Initialise the spatial domain $x = [0, L]$ with Nx points
Set $u(x, 0)$ based on the initial displacement profile $f(x)$
Numerical Scheme (Finite Difference):
for n from 1 to $Nt - 1$ **do**
    for i from 1 to $Nx - 1$ **do**
        Update $u(i, n + 1)$ using the central difference scheme:
        $u(i, n + 1) = 2 \cdot u(i, n) - u(i, n - 1) + (dt^2) \cdot \left(\frac{dx^2}{L^2}\right) \cdot (u(i + 1, n) - 2 \cdot u(i, n) + u(i - 1, n))$
    end for
end for
Visualisation:
Create plots to visualise the wave propagation:
for selected time steps (e.g., every 50 time steps) **do**
    Plot $u(x, t)$ for the current time step
    Add an annotation with the corresponding time value
end for
Display the plots to visualise the wave evolution

Appendix 2

To show the equation in (16) **holds, we apply the identity** $\sin^2(\theta) = \frac{1}{2} - \frac{1}{2}\cos(2\theta)$**.**

$$\int_0^L B_m \sin^2\left(\frac{m\pi x}{L}\right) dx = \frac{L}{2} B_m$$

$$\begin{aligned}
\int_0^L B_m \sin^2\left(\frac{m\pi x}{L}\right) dx &= \int_0^L B_m \left(\frac{1}{2} - \frac{1}{2}\cos\left(\frac{2m\pi x}{L}\right)\right) dx \\
&= \frac{B_m}{2} \int_0^L \left(1 - \cos\left(\frac{2m\pi x}{L}\right)\right) dx \\
&= \frac{B_m}{2} \left[x - \frac{L}{2m\pi}\sin\left(\frac{2m\pi x}{L}\right)\right]_0^L \\
&= \frac{B_m}{2} \int_0^L (1 - \cos\left(\frac{2m\pi x}{L}\right)) \, dx \\
&= \frac{B_m}{2} \left[x - \frac{L}{2m\pi}\sin\left(\frac{2m\pi x}{L}\right)\right]_0^L \\
&= \frac{B_m}{2} \left[L - \frac{L}{2m\pi}\sin\left(\frac{2m\pi L}{L}\right) - 0 + \frac{L}{2m\pi}\sin\left(\frac{2m\pi \cdot 0}{L}\right)\right] \\
&= \frac{B_m}{2} \left[L - \frac{L}{2m\pi}\sin(2m\pi) + \frac{L}{2m\pi}\sin(0)\right] \\
&= \frac{B_m}{2} \left[L - \frac{L}{2m\pi} \cdot 0 + \frac{L}{2m\pi} \cdot 0\right] \\
&= \frac{L}{2} B_m
\end{aligned}$$